New behaviors of α-particle preformation factors near doubly magic 100Sn

Jungang Deng
Lanzhou University
Xiaodong Sun
China institute of Atomic Energy
Hongfei Zhang (zhanghf@xjtu.edu.cn)
XI'an Jiaotong University https://orcid.org/0000-0003-0326-5701

Research Article

Keywords: preformation factors, doubly magic nuclei, proton-neutron interaction, Alpha-decay half-lives

Posted Date: December 3rd, 2021

DOI: https://doi.org/10.21203/rs.3.rs-1121549/v1

New behaviors of α-particle preformation factors near doubly magic ^{100}Sn

Jun-Gang Deng,[1,2] Hong-Fei Zhang,[1,*] and Xiao-Dong Sun[3]

[1] *School of Physics, Xi'an Jiaotong University, 710049 Xi'an, People's Republic of China*
[2] *School of Nuclear Science and Technology, Lanzhou University, 730000 Lanzhou, People's Republic of China*
[3] *China Nuclear Data Center, China Institute of Atomic Energy, P.O. Box 275(41), 102413 Beijing, People's Republic of China*

The α-particle preformation factors of nuclei above doubly magic nuclei ^{100}Sn and ^{208}Pb are investigated. The results show that the α-particle preformation factors of nuclei near self-conjugate doubly magic ^{100}Sn are larger significantly than those of analogous nuclei just above ^{208}Pb, and they will be enhanced as the nuclei move towards the $N = Z$ line. The correlation energy of the proton-neutron E_{p-n} and two protons-two neutrons E_{2p-2n} of nuclei near ^{100}Sn also exhibit similar situations indicating that the interactions between protons and neutrons occupying similar single-particle orbitals could enhance the α-particle preformation factors and result in the superallowed α decay. It also provides evidence of the significant role of proton-neutron interaction on α-particle preformation. Besides, the linear relationship between α-particle preformation factors and the product of valence protons and valence neutrons for nuclei around ^{208}Pb is broken in the ^{100}Sn region because the α-particle preformation factor is enhanced when the nucleus near ^{100}Sn moves towards the $N = Z$ line. Furthermore, the calculated α decay half-lives can well reproduce the experimental data including the recent observed self-conjugate nuclei ^{104}Te and ^{108}Xe [Phys. Rev. Lett. 121, 182501 (2018)].

α decay is a fundamental nuclear decay mode. The researches on α decay have long been focused on the vicinities of doubly magic nuclei ^{208}Pb ($Z = 82, N = 126$) and ^{298}Fl ($Z = 114, N = 184$) because α decay can be a probe to study the unstable nucleus structure, and can be the only way to identify the new synthesized superheavy nucleus [1–27]. Over the past two decades, the α emitters around the self-conjugate doubly magic nucleus ^{100}Sn ($Z = N = 50$) at the opposite end of the mass table have also received a lot of attention and become a hot topic in nuclear physics [18, 28–35]. In particular, there is the fastest α emitter ^{104}Te near doubly magic nucleus ^{100}Sn [34]. Since the α emitters near self-conjugate doubly magic nucleus ^{100}Sn are close to the $N = Z$ line, the nuclear force is extremely sensitive to isospin. Therefore, it is a great chance to study and obtain the unique neutron-deficient nuclear structure information and examine various α decay theoretical models. Moreover, the cluster radioactivity was also predicted as one of the decay modes of the nucleus in the ^{100}Sn region [36–39]. Further interest in the decay rates of nuclei around doubly magic nucleus ^{100}Sn comes from the research of astrophysical processes, for which this region has been considered as the end of the rapid proton capture process due to the Sn-Sb-Te cycle [33, 40, 41].

In addition, in the neutron-deficient Te, Xe, and Ba isotopes near ^{100}Sn, one would expect that the interactions between protons and neutrons occupying similar single-particle orbitals could enhance the α-particle preformation factors and the reduced α-widths significantly when compared to the analogous nuclei just above doubly magic nucleus ^{208}Pb, and result in the so-called "superallowed" α decay [42]. And this effect would be expected to be the greatest for the $N = Z$ self-conjugate nuclei [42]. Recently, the first time α radioactivity to a heavy self-conjugate nucleus was observed on the ^{108}Xe$\rightarrow^{104}$Te$\rightarrow^{100}$Sn α decay chain [34], including the measurements of the α-particle kinetic energy and α decay half-lives of the α emitters ^{108}Xe [$E_\alpha = 4.4(2)$ MeV, $T_{1/2} = 58^{+106}_{-23}$ μs] and ^{104}Te [$E_\alpha = 4.9(2)$ MeV, $T_{1/2} < 18$ ns]. The authors of this reference suggested that the α-reduced width for ^{108}Xe or ^{104}Te is more than a factor of 5 larger than that for ^{212}Po [34].

It is well known that ^{104}Te, near the proton drip line, and ^{212}Po, near the $\beta-$stability line, are the only two existing α emitters decaying to the doubly magic nuclei. In this work, we focus on the α-particle preformation factors of nuclei near self-conjugate doubly magic nucleus ^{100}Sn and compare them to those of analogous nuclei just above the doubly magic nucleus ^{208}Pb based on the available experimental data of α decay [34, 43–53] within the generalized liquid drop model (GLDM) [54–60]. These α emitters are in different isospins and mass numbers as well as around different protons and neutrons closed shells. We want to reveal some new behaviors of α-particle preformation factors of extremely neutron-deficient nuclei near self-conjugate doubly magic nucleus ^{100}Sn for understanding the roles of proton-neutron correlation and the single-particle orbitals occupied by protons and neutrons in the preformation of α-cluster as well as the physical mechanism of superallowed α decay.

The GLDM can well deal with proton radioactivity [61], cluster radioactivity [62], fusion [63], fission [64], and the α decay process [22, 54–60, 65] because of introducing the quasimolecular shape mechanism [54], which can describe the complex deformation process from the parent nucleus continuous transition to the appearance of a deep and narrow neck finally resulting in two tangential fragments, and adding the proximity energy, including an

* zhanghongfei@lzu.edu.cn

accurate radius and mass asymmetry. In previous works [54–60], the GLDM has been discussed in detail. The α decay half-life can be obtained by

$$T_{1/2} = \frac{\ln 2}{\lambda}, \tag{1}$$

with the α decay constant λ being expressed as

$$\lambda = P_\alpha \nu P, \tag{2}$$

where the assault frequency ν is obtained by using the classical method with the kinetic energy of the α-particle. The barrier penetrating probability P is determined by tunneling the GLDM potential barriers [54–60] with the Wentzel-Kramers-Brillouin (WKB) approximation.

The experimental α-particle preformation factor $P_\alpha^{\rm Exp}$ can be extracted from the ratios between the theoretical decay half-life $T_{1/2}^{\rm Cal1}$ calculated by assuming the α-particle preformation factor as a constant $P_\alpha = 1$ to experimental data [59, 66–69] and expressed as

$$P_\alpha^{\rm Exp} = \frac{T_{1/2}^{\rm Cal1}}{T_{1/2}^{\rm Exp}}. \tag{3}$$

To examine the experimental α decay half-life data, the analytic formula for estimating the α-particle preformation factor is also adopted, which is put forward in our previous work [60, 65]. It is expressed as

$$\log_{10} P_\alpha^{\rm Eq} = a + bA^{1/6}\sqrt{Z} + c\frac{Z}{\sqrt{Q_\alpha}} - d\chi' - e\rho' + f\sqrt{l(l+1)}, \tag{4}$$

where $\chi' = Z_1 Z_2 \sqrt{\frac{A_1 A_2}{(A_1+A_2)Q_\alpha}}$ and $\rho' = \sqrt{\frac{A_1 A_2}{A_1+A_2} Z_1 Z_2 (A_1^{1/3} + A_2^{1/3})}$. A, Z, and Q_α represent mass number, proton number, and α decay energy of the parent nucleus. A_1, Z_1, A_2, and Z_2 denote the mass and proton numbers of the α-particle and daughter nucleus. l is the angular momentum carried by the α-particle. The parameters values are listed in Ref. [60].

The calculated α decay half-lives for nuclei above doubly magic nuclei ^{100}Sn and ^{208}Pb are presented in Tables I and II, respectively. In these two tables, the first four columns represent the α transition, the experimental kinetic energy of the α-particle, the experimental α decay energy, and the minimum angular momentum carried by the α-particle. The fifth column is the experimental α decay half-life. The sixth column denotes the calculated α decay half-life $T_{1/2}^{\rm Cal1}$ within the GLDM with $P_\alpha = 1$. The seventh column gives the calculated α decay half-life $T_{1/2}^{\rm Cal2}$ within the GLDM with the estimated α-particle preformation factor from Eq. (4). The eighth column shows the extracted experimental α-particle preformation factor by using Eq. (3) with $T_{1/2}^{\rm Cal1}$ and $T_{1/2}^{\rm Exp}$. The last two columns express the calculated correlation energy of the proton-neutron E_{p-n} and two protons-two neutrons E_{2p-2n} determined by Eqs. (6) and (7). From these two tables, it can be seen immediately that the calculated α decay half-lives $T_{1/2}^{\rm Cal2}$ can well reproduce the experimental data including the newly observed self-conjugate nuclei ^{104}Te and ^{108}Xe [34]. Note that the calculations provide supports for recent experimental observation data in Ref. [34]. To measure the agreements between the calculated α decay half-lives $T_{1/2}^{\rm Cal2}$ and experimental data $T_{1/2}^{\rm Exp}$, the standard deviations are calculated by

$$\sigma = \sqrt{\frac{1}{n}\sum (\log_{10} T_{1/2}^{\rm Cal2} - \log_{10} T_{1/2}^{\rm Exp})^2}. \tag{5}$$

For nuclei in Tables I and II, the results of standard deviations $\sigma_1 = 0.47$ and $\sigma_2 = 0.16$ are satisfactory manifesting that $T_{1/2}^{\rm Cal2}$ can well reproduce $T_{1/2}^{\rm Exp}$ within factors of $10^{0.47} = 2.95$ and $10^{0.16} = 1.45$, respectively. It demonstrated that the GLDM can be applied to extract the experimental α-particle preformation factors for studying the structure information of nuclei in these two regions.

Furthermore, in Tables I and II, we can see that the extracted experimental α-particle preformation factors $P_\alpha^{\rm Exp}$ of nuclei near ^{100}Sn are larger than $P_\alpha^{\rm Exp}$ of nuclei near ^{208}Pb, and in particular, larger than $P_\alpha^{\rm Exp}$ of analogous nuclei just above ^{208}Pb. The analogous nuclei refer to the two nuclei with the same valence proton and valence neutron located above doubly magic cores ^{100}Sn and ^{208}Pb, respectively. The valence protons N_p and valence neutrons N_n are defined as $N_p = Z - Z_0$ and $N_n = N - N_0$ with $Z_0 = 50$ and 82, as well as $N_0 = 50$ and 126, being the magic numbers of protons and neutrons in the corresponding nuclear region. For example, ^{104}Te is analogous to ^{212}Po because they both have two valence protons and two valence neutrons outside of the doubly magic nuclei ^{100}Sn and ^{208}Pb, respectively.

The extracted experimental α-particle preformation factors $P_\alpha^{\rm Exp}$ for nuclei above ^{100}Sn and for analogous nuclei just above ^{208}Pb are shown as functions of valence protons and valence neutrons in Fig. 1 (a), (b), and (c), respectively. In this figure, one can see that the $P_\alpha^{\rm Exp}$ of nuclei above ^{100}Sn are significantly larger than those of analogous nuclei just above ^{208}Pb. Furthermore, Fig. 1 (a) shows the variations of $P_\alpha^{\rm Exp}$ for Te ($Z = 52$) and Po ($Z = 84$) isotopes, whose valence protons are $N_p = Z - Z_0 = 2$, against valence neutrons N_n. It is clearly seen that for Te isotopes the $P_\alpha^{\rm Exp}$ exhibits an increasing trend when the nucleus moves towards the $N = Z$ line, but the $P_\alpha^{\rm Exp}$ of Po isotopes do not show similar patterns due to the large asymmetry between neutrons and protons. Fig. 1 (b) displays the variations of $P_\alpha^{\rm Exp}$ for Xe ($Z = 54$) and Rn ($Z = 86$) isotopes, whose valence protons are $N_p = Z - Z_0 = 4$, against valence neutrons N_n. We can find that for Xe isotopes the $P_\alpha^{\rm Exp}$ also increases as the nucleus moves towards the $N = Z$ line. However, the $P_\alpha^{\rm Exp}$ of Rn isotopes still do not show a similar trend of change. Fig. 1 (c) plots the $P_\alpha^{\rm Exp}$ as functions of valence protons N_p for $N = 58$ and $N = 134$ isotones, whose valence neutrons are $N_n = N - N_0 = 8$.

TABLE I. Calculations of α-particle preformation factor, α decay half-lives, and the correlation energy of the proton-neutron E_{p-n} and two protons-two neutrons E_{2p-2n} of even-even Te, Xe, and Ba isotopes near ^{100}Sn.

α transition	E_α (MeV)	Q_α (MeV)	l_{min}	$T_{1/2}^{\rm Exp}$ (s)	$T_{1/2}^{\rm Cal1}$ (s)	$T_{1/2}^{\rm Cal2}$ (s)	$P_\alpha^{\rm Exp}$	E_{p-n} (MeV)	E_{2p-2n} (MeV)
^{104}Te$\rightarrow^{100}$Sn	4.9 [34]	5.1	0	$< 1.80 \times 10^{-8}$ [34]	1.47×10^{-8}	7.29×10^{-8}	> 0.81	1.26[a]	3.64[a]
^{106}Te$\rightarrow^{102}$Sn	4.128 [45]	4.29	0	7.00×10^{-5} [44–46]	2.52×10^{-5}	8.38×10^{-5}	0.36	0.56[b]	1.84[a]
^{108}Te$\rightarrow^{104}$Sn	3.314 [48]	3.44	0	4.30×10^{0} [45, 47, 48]	9.30×10^{-1}	1.68×10^{0}	0.22	1.06[b]	1.83[b]
^{110}Te$\rightarrow^{106}$Sn	2.624 [49]	2.72	0	2.78×10^{6} [49, 50]	3.32×10^{5}	2.87×10^{5}	0.12	0.71[b]	1.73[b]
^{108}Xe$\rightarrow^{104}$Te	4.32 [34, 43]	4.49	0	5.80×10^{-5} [34]	3.70×10^{-5}	1.10×10^{-4}	0.64	1.10[a]	3.35[a]
^{110}Xe$\rightarrow^{106}$Te	3.72 [44]	3.86	0	1.48×10^{-1} [44]	5.00×10^{-2}	1.07×10^{-1}	0.34	0.73[b]	2.02[a]
^{112}Xe$\rightarrow^{108}$Te	3.216 [45]	3.34	0	3.38×10^{2} [45, 47]	1.01×10^{2}	1.53×10^{2}	0.30	1.13[b]	1.66[b]
^{114}Ba$\rightarrow^{110}$Xe	3.48 [44]	3.61	0	4.20×10^{1} [44]	2.60×10^{1}	4.19×10^{1}	0.62	0.66[b]	1.96[a]

[a] It is calculated by using the nuclear mass data in the WS4+ mass model [70].
[b] It is calculated by using the nuclear mass data in the evaluated atomic mass table AME2016 [52, 53].

TABLE II. Same as Table I, but for even-even Po, Rn, and Ra isotopes near ^{208}Pb. The experimental α decay half-lives are taken from the evaluated nuclear properties table NUBASE2016 [51]. The experimental α decay energy are taken from the evaluated atomic mass table AME2016 [52, 53]. The E_{p-n} energy and E_{2p-2n} energy are calculated by using the nuclear mass data in the AME2016 [52, 53].

α transition	E_α (MeV)	Q_α (MeV)	l_{min}	$T_{1/2}^{\rm Exp}$ (s)	$T_{1/2}^{\rm Cal1}$ (s)	$T_{1/2}^{\rm Cal2}$ (s)	$P_\alpha^{\rm Exp}$	E_{p-n} (MeV)	E_{2p-2n} (MeV)
^{212}Po$\rightarrow^{208}$Pb	8.79	8.95	0	2.95×10^{-7}	1.00×10^{-8}	1.48×10^{-7}	0.03	0.87	1.44
^{214}Po$\rightarrow^{210}$Pb	7.69	7.83	0	1.64×10^{-4}	1.14×10^{-5}	1.23×10^{-4}	0.07	0.70	1.28
^{216}Po$\rightarrow^{212}$Pb	6.78	6.91	0	1.45×10^{-1}	1.39×10^{-2}	1.09×10^{-1}	0.10	0.51	1.11
^{218}Po$\rightarrow^{214}$Pb	6.00	6.12	0	1.86×10^{2}	1.93×10^{1}	1.09×10^{2}	0.10	0.38	1.09
^{212}Rn$\rightarrow^{208}$Po	6.26	6.38	0	1.43×10^{3}	1.40×10^{1}	6.86×10^{2}	0.01	0.23	0.57
^{214}Rn$\rightarrow^{210}$Po	9.04	9.21	0	2.70×10^{-7}	1.08×10^{-8}	1.85×10^{-7}	0.04	0.67	1.24
^{216}Rn$\rightarrow^{212}$Po	8.05	8.20	0	4.50×10^{-5}	4.99×10^{-6}	6.56×10^{-5}	0.11	0.70	1.33
^{218}Rn$\rightarrow^{214}$Po	7.13	7.26	0	3.38×10^{-2}	4.23×10^{-3}	4.15×10^{-2}	0.13	0.58	1.29
^{220}Rn$\rightarrow^{216}$Po	6.29	6.41	0	5.56×10^{1}	8.33×10^{0}	5.92×10^{1}	0.15	0.52	1.18
^{222}Rn$\rightarrow^{218}$Po	5.49	5.59	0	3.30×10^{5}	5.71×10^{4}	2.79×10^{5}	0.17	0.51	1.15
^{214}Ra$\rightarrow^{210}$Rn	7.14	7.27	0	2.44×10^{0}	3.25×10^{-2}	1.53×10^{0}	0.01	0.22	0.65
^{216}Ra$\rightarrow^{212}$Rn	9.35	9.53	0	1.82×10^{-7}	8.41×10^{-9}	1.70×10^{-7}	0.05	0.52	1.14
^{218}Ra$\rightarrow^{214}$Rn	8.39	8.55	0	2.52×10^{-5}	2.44×10^{-6}	3.88×10^{-5}	0.10	0.58	1.21
^{220}Ra$\rightarrow^{216}$Rn	7.45	7.59	0	1.79×10^{-2}	1.93×10^{-3}	2.34×10^{-2}	0.11	0.68	1.35
^{222}Ra$\rightarrow^{218}$Rn	6.56	6.68	0	3.36×10^{1}	4.46×10^{0}	3.92×10^{1}	0.13	0.44	1.34
^{224}Ra$\rightarrow^{220}$Rn	5.69	5.79	0	3.14×10^{5}	4.97×10^{4}	2.99×10^{5}	0.16	0.41	1.25
^{226}Ra$\rightarrow^{222}$Rn	4.78	4.87	0	5.05×10^{10}	1.10×10^{10}	4.00×10^{10}	0.22	0.40	1.23

The $P_\alpha^{\rm Exp}$ of $N = 58$ isotones also show an increasing tendency as the nuclei move towards the $N = Z$ line, but this phenomenon has not occurred in the analogous $N = 134$ isotopes just above ^{208}Pb. It is indicated that the $P_\alpha^{\rm Exp}$ is enhanced when a nucleus moves towards the $N = Z$ line, and result in the superallowed α decay near doubly magic nucleus ^{100}Sn. In recent work, Clark et al. adopted a very different model and studied the α-particle preformation factors of nuclei in these two regions [31]. A similar conclusion was obtained though the α-particle

preformation factors of nuclei near doubly magic nuclei ^{100}Sn and ^{208}Pb are in orders of 10^{-2} and 10^{-3}, respectively.

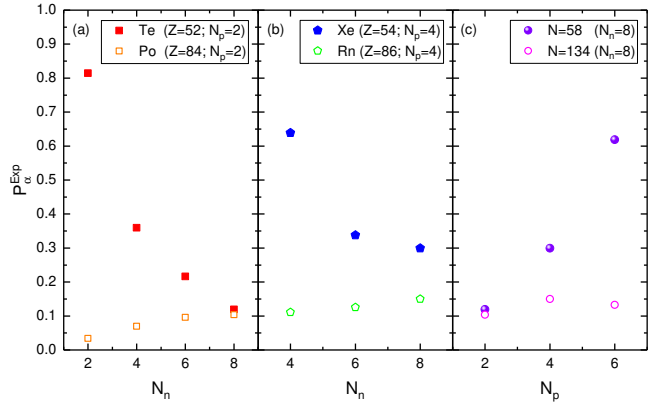

FIG. 1. (Color online) The variations of extracted experimental α-particle preformation factors $P_\alpha^{\rm Exp}$ from Eq. (3) against the valence neutrons for $Z = 52$ and $Z = 84$ isotopes (left), and against the valence neutrons for $Z = 54$ and $Z = 86$ isotopes (middle), and against the valence protons for $N = 58$ and $N = 134$ isotones (right), respectively.

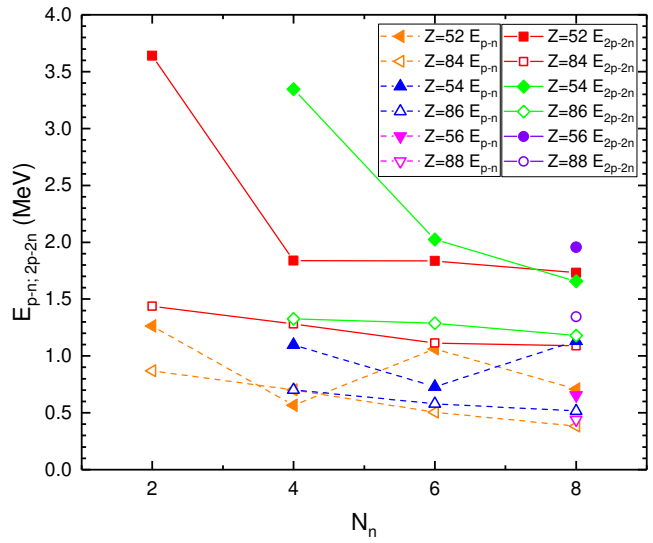

FIG. 2. (Color online) The correlation energy of the proton-neutron E_{p-n} and two protons-two neutrons E_{2p-2n} of nuclei above ^{100}Sn (denoted as solid symbols) and those of analogous nuclei just above ^{208}Pb (denoted as open symbols).

For investigating the effects of proton-neutron interaction and two protons-two neutrons interaction on the α-particle preformation, we calculate the correlation energy of the proton-neutron E_{p-n} and two protons-two neutrons E_{2p-2n} using

$$\begin{aligned} E_{p-n} =& B(A,Z) + B(A-2,Z-1) \\ & - B(A-1,Z-1) - B(A-1,Z), \end{aligned} \tag{6}$$

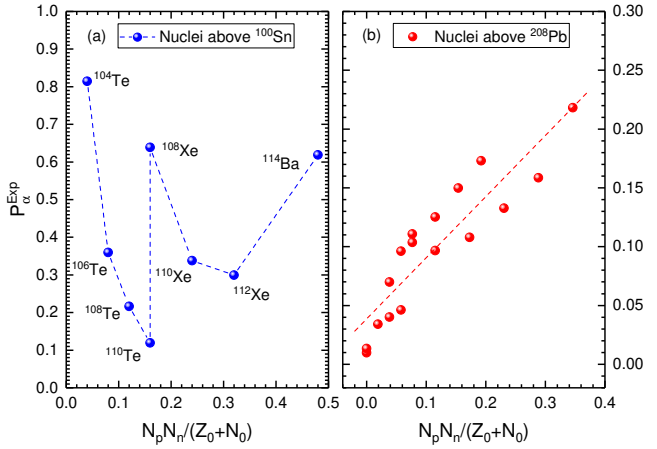

FIG. 3. (Color online) The variations of extracted experimental α-particle preformation factors $P_\alpha^{\rm Exp}$ from Eq. (3) against $\frac{N_pN_n}{Z_0+N_0}$ for nuclei above ^{100}Sn (left) and for nuclei above ^{208}Pb (right), respectively.

$$\begin{aligned} E_{2p-2n} =& B(A,Z) + B(A-4,Z-2) \\ & - B(A-2,Z-2) - B(A-2,Z). \end{aligned} \tag{7}$$

Eqs. (6) and (7) were proposed in Ref. [71] and used to determine the experimental pairing energy of the nucleons [72]. $B(A, Z)$ is the binding energy of a nucleus with the mass number A and proton number Z. The results of E_{p-n} energy and E_{2p-2n} energy are listed in the last two columns of Tables I and II. In these two tables, it can be found that the E_{p-n} energy and E_{2p-2n} energy of nuclei above doubly magic nucleus ^{100}Sn are larger than those of analogous nuclei just above ^{208}Pb. This, in turn, leads to that the $P_\alpha^{\rm Exp}$ of nuclei near ^{100}Sn are enhanced significantly. The results of E_{p-n} energy and E_{2p-2n} energy are plotted in Fig. 2. In this figure, the E_{p-n} energy and E_{2p-2n} energy of nuclei above ^{100}Sn are strengthened when compared to analogous nuclei just above ^{208}Pb. For $Z = 52$ isotopes, the E_{p-n} energy and E_{2p-2n} energy increase rapidly in $N_n = 2$. Similarly, for $Z = 54$ isotopes, the E_{p-n} energy and E_{2p-2n} energy rise fast in $N_n = 4$. However, the E_{p-n} energy and E_{2p-2n} energy of analogous nuclei just above ^{208}Pb are changed slowly. Therefore, it demonstrated that the α-particle is more to form in self-conjugate nuclei and result in the superallowed α decay. In addition, the E_{2p-2n} energy appears an increased tendency, the same as $P_\alpha^{\rm Exp}$, when the nucleus moves towards the $N = Z$ line implying that the two protons-two neutrons interaction play a more significant role than one proton-one neutron interaction in α-particle preformation.

The extracted experimental α-particle preformation factors $P_\alpha^{\rm Exp}$ for nuclei above ^{100}Sn and ^{208}Pb are shown as functions of $\frac{N_pN_n}{Z_0+N_0}$ in Fig. 3 (a) and (b), respectively. In Fig. 3 (b), one can see that the closer the $\frac{N_pN_n}{Z_0+N_0}$ is to the zero, representing the proton and/or neutron num-

bers approaches the closed shells, the smaller $P_\alpha^{\rm Exp}$ is. When the $\frac{N_pN_n}{Z_0+N_0}$ is far from zero, the $P_\alpha^{\rm Exp}$ will increase. This indicates that the closer the proton and/or neutron number is to the magic number, the more difficult it is for an α-particle to form inside its parent nucleus. And we can find that the $P_\alpha^{\rm Exp}$ is linearly dependent on the $\frac{N_pN_n}{Z_0+N_0}$ for nuclei above ^{208}Pb. It is consistent with the conclusions deduced by adopting the different models, in which the α-particle preformation factors are extracted from the ratios between theoretical α decay half-lives calculated by adopting the different models to experimental data [15, 73, 74], or calculated using the differences of binding energy between the α decaying parent nucleus and its neighboring nuclei within the cluster-formation model [75]. It is shown that the nuclear shell effects and the nucleons configuration play key roles in α-cluster preformation for α-particle emitters around doubly magic ^{208}Pb. However, in Fig. 3 (a) this phenomenon is broken in the ^{100}Sn region. The $P_\alpha^{\rm Exp}$ of nuclei above ^{100}Sn are linearly independent of $\frac{N_pN_n}{Z_0+N_0}$ and show a new behavior. When the nucleus is close to the shell closures, the $P_\alpha^{\rm Exp}$ of the nucleus near ^{100}Sn does not decrease like that of the nucleus near ^{208}Pb, but it increases. In addition, we can find that the maximum values of the $P_\alpha^{\rm Exp}$ in Fig. 3 (a) correspond to ^{104}Te, ^{108}Xe, and ^{114}Ba. In particular along the $N = Z$ line, the $P_\alpha^{\rm Exp}$ is significantly enhanced, which results in the $P_\alpha^{\rm Exp}$ of nuclei above ^{100}Sn are not linearly dependent on $\frac{N_pN_n}{Z_0+N_0}$.

In summary, we systematically study the α-particle preformation factors $P_\alpha^{\rm Exp}$ of nuclei above doubly magic nuclei ^{100}Sn and ^{208}Pb, which are extracted from the ratios between the theoretical α-decay half-lives within the GLDM to experimental data. The results show that the $P_\alpha^{\rm Exp}$ of nuclei near self-conjugate doubly magic ^{100}Sn are larger significantly than those of analogous nuclei just above ^{208}Pb, and they will be enhanced when the nucleus moves towards the $N = Z$ line. The correlation energy of proton-neutron E_{p-n} and two protons-two neutrons E_{2p-2n} of nuclei near ^{100}Sn are also larger than those of analogous nuclei just above ^{208}Pb. It is indicated that the interactions between protons and neutrons occupying similar single-particle orbitals could enhance the $P_\alpha^{\rm Exp}$ and result in the superallowed α decay near doubly magic nucleus ^{100}Sn. Furthermore, as the nucleus moves towards the $N = Z$ line, the E_{2p-2n} energy shows an increased tendency which is the same as that of $P_\alpha^{\rm Exp}$, while E_{p-n} energy doesn't appear this pattern, indicating E_{2p-2n} energy plays a more important role than E_{p-n} energy in α-particle preformation of superallowed α decay. The linear relationship between the $P_\alpha^{\rm Exp}$ and the product of valence protons and valence neutrons $\frac{N_pN_n}{Z_0+N_0}$ for nuclei above ^{208}Pb is broken in the ^{100}Sn region because the $P_\alpha^{\rm Exp}$ is enhanced when the nucleus near ^{100}Sn moves towards the $N = Z$ line. Besides, the calculated α decay half-lives can well reproduce experimental data including the newly observed self-conjugate nuclei ^{108}Xe and ^{104}Te. This work also provides evidence of the significant role of proton-neutron interaction on the α-particle preformation, which will shed some new light on α decay and α-particle preformation factors researches of nuclear physics in the future.

This work is supported by National Natural Science Foundation of China (Grants No. 12175170, No. 11675066, No. 11665019).

[1] D.F. Geesaman *et al.* Physics of a rare isotope accelerator. *Annu. Rev. Nucl. Part. Sci.* **56**, 53–92 (2006).

[2] S. Hofmann and G. Münzenberg. The discovery of the heaviest elements. *Rev. Mod. Phys.* **72**, 733–767 (2000).

[3] M. Pfützner *et al.* Radioactive decays at limits of nuclear stability. *Rev. Mod. Phys.* **84**, 567–619 (2012).

[4] A. N. Andreyev *et al.* Signatures of the Z=82 shell closure in α-decay process. *Phys. Rev. Lett.* **110**, 242502 (2013).

[5] L. Ma *et al.* α-decay properties of the new isotope ^{216}U. *Phys. Rev. C* **91**, 051302(R) (2015).

[6] Chong Qi, Roberto Liotta, and Ramon Wyss. Recent developments in radioactive charged-particle emissions and related phenomena. *Prog. Part. Nucl. Phys.* **105**, 214 – 251 (2019).

[7] B. Buck, A. C. Merchant, and S. M. Perez. New look at α decay of heavy nuclei. *Phys. Rev. Lett.* **65**, 2975–2977 (1990).

[8] B. Buck, A. C. Merchant, and S. M. Perez. Alpha-cluster structure in ^{212}Po. *Phys. Rev. Lett.* **72**, 1326–1328 (1994).

[9] A. Astier *et al.* Novel manifestation of α-clustering structures: New "$\alpha+^{208}$ Pb" states in ^{212}Po revealed by their enhanced $e1$ decays. *Phys. Rev. Lett.* **104**, 042701 (2010).

[10] J. W. Beeman *et al.* First measurement of the partial widths of ^{209}Bi decay to the ground and to the first excited states. *Phys. Rev. Lett.* **108**, 062501 (2012).

[11] Pierre de Marcillac *et al.* Experimental detection of α-particles from the radioactive decay of natural bismuth. *Nature* **422**, 876 – 878 (2003).

[12] Z. Y. Zhang *et al.* New isotope ^{220}Np: Probing the robustness of the $n = 126$ shell closure in neptunium. *Phys. Rev. Lett.* **122**, 192503 (2019).

[13] L. Ma *et al.* Short-lived α-emitting isotope ^{222}Np and the stability of the $N = 126$ magic shell. *Phys. Rev. Lett.* **125**, 032502 (2020).

[14] M.D. Sun *et al.* New short-lived isotope ^{223}Np and the absence of the $Z = 92$ subshell closure near $N = 126$. *Phys. Lett. B* **771**, 303 – 308 (2017).

[15] W. M. Seif, M. Shalaby, and M. F. Alrakshy. Isospin asymmetry dependence of the α spectroscopic factor for heavy nuclei. *Phys. Rev. C* **84**, 064608 (2011).

[16] Yuejiao Ren and Zhongzhou Ren. New geiger-nuttall law for α decay of heavy nuclei. *Phys. Rev. C* **85**, 044608 (2012).

[17] Chang Xu *et al.* α-cluster formation and decay in the

quartetting wave function approach. *Phys. Rev. C* **95**, 061306(R) (2017).
[18] Shuo Yang *et al.* α decay to a doubly magic core in the quartetting wave function approach. *Phys. Rev. C* **101**, 024316 (2020).
[19] Zhen Wang, Zhongzhou Ren, and Dong Bai. Theoretical studies on α-decay half-lives of $N = 125, 126,$ and127 isotones. *Phys. Rev. C* **101**, 054310 (2020).
[20] Jun-Gang Deng, Hong-Fei Zhang, and G. Royer. Improved empirical formula for α-decay half-lives. *Phys. Rev. C* **101**, 034307 (2020).
[21] Jun-Gang Deng and Hong-Fei Zhang. Systematic study of α decay half-lives within the generalized liquid drop model with various versions of proximity energies. *Chin. Phys. C* **45**, 024104 (2021).
[22] Na-Na Ma, Xiao-Jun Bao, and Hong-Fei Zhang. Diffuseness effect and radial basis function network for optimizing α decay calculations. *Chin. Phys. C* **45**, 024105 (2021).
[23] Yi-Bin Qian and Zhong-Zhou Ren. New look at geiger-nuttall law and α clustering of heavy nuclei. *Chin. Phys. C* **45**, 021002 (2021).
[24] Wei Hua *et al.* Fine structure of α decay in ^{222}Pa. *Chin. Phys. C* **45**, 044001 (2021).
[25] Yan He, Xuan Yu, and Hong-Fei Zhang. Improved empirical formula for α particle preformation factor. *Chin. Phys. C* **45**, 014110 (2021).
[26] Y. Z. Wang, J. M. Dong, B. B. Peng, and H. F. Zhang. Fine structure of α decay to rotational states of heavy nuclei. *Phys. Rev. C* **81**, 067301 (2010).
[27] Y. Z. Wang, S. J. Wang, Z. Y. Hou, and J. Z. Gu. Systematic study of α-decay energies and half-lives of superheavy nuclei. *Phys. Rev. C* **92**, 064301 (2015).
[28] Chang Xu and Zhongzhou Ren. Half lives of α-emitters approaching the $N = Z$ line. *Phys. Rev. C* **74**, 037302 (2006).
[29] Monika Patial, R. J. Liotta, and R. Wyss. Microscopic description of superallowed α-decay transitions. *Phys. Rev. C* **93**, 054326 (2016).
[30] Y. Xiao *et al.* Search for α decay of ^{104}Te with a novel recoil-decay scintillation detector. *Phys. Rev. C* **100**, 034315 (2019).
[31] R. M. Clark *et al.* Enhancement of α-particle formation near ^{100}Sn. *Phys. Rev. C* **101**, 034313 (2020).
[32] F. Mercier *et al.* Microscopic description of the self-conjugate ^{108}Xe and ^{104}Te α-decay chain. *Phys. Rev. C* **102**, 011301 (2020).
[33] S. N. Liddick *et al.* Discovery of ^{109}Xe and ^{105}Te: Superallowed α decay near doubly magic ^{100}Sn. *Phys. Rev. Lett.* **97**, 082501 (2006).
[34] K. Auranen *et al.* Superallowed α decay to doubly magic ^{100}Sn. *Phys. Rev. Lett.* **121**, 182501 (2018).
[35] P. Arthuis, C. Barbieri, M. Vorabbi, and P. Finelli. Ab initio computation of charge densities for Sn and Xe isotopes. *Phys. Rev. Lett.* **125**, 182501 (2020).
[36] Satish Kumar and Raj K. Gupta. Measurable decay modes of barium isotopes via exotic cluster emissions. *Phys. Rev. C* **49**, 1922–1926 (1994).
[37] Satish Kumar, Dharam Bir, and Raj K. Gupta. ^{100}Sn – daughter α-nuclei cluster decays of some neutron-deficient Xe to Gd parents: Sn radioactivity. *Phys. Rev. C* **51**, 1762–1771 (1995).
[38] A. Florescu and A. Insolia. Microscopic calculation for α and heavier cluster emissions from proton rich ba and ce isotopes. *Phys. Rev. C* **52**, 726–732 (1995).
[39] H. F. Zhang *et al.* Preformation of clusters in heavy nuclei and cluster radioactivity. *Phys. Rev. C* **80**, 037307 (2009).
[40] H. Schatz *et al.* rp-process nucleosynthesis at extreme temperature and density conditions. *Phys. Rep.* **294**, 167 – 263 (1998).
[41] H. Schatz *et al.* End point of the *rp* process on accreting neutron stars. *Phys. Rev. Lett.* **86**, 3471–3474 (2001).
[42] Ronald D. Macfarlane and Antti Siivola. New region of alpha radioactivity. *Phys. Rev. Lett.* **14**, 114–115 (1965).
[43] National Nuclear Data Center, URL: https://www.nndc.bnl.gov/
[44] L. Capponi *et al.* Direct observation of the ^{114}Ba $\rightarrow^{110}$ Xe $\rightarrow^{106}$ Te $\rightarrow^{102}$ Sn triple α-decay chain using position and time correlations. *Phys. Rev. C* **94**, 024314 (2016).
[45] R. D. Page *et al.* Alpha radioactivity above ^{100}Sn including the decay of ^{108}I. *Phys. Rev. C* **49**, 3312–3315 (1994).
[46] C. Mazzocchi *et al.* Alpha decay of ^{114}Ba. *Phys. Lett. B* 532, 29 – 36 (2002).
[47] D. Schardt *et al.* Alpha decay studies of tellurium, iodine, xenon and cesium isotopes. *Nucl. Phys. A* **326**, 65 – 82 (1979).
[48] F. Heine *et al.* Proton and alpha radioactivity of very neutron deficient Te, I, Xe and Cs isotopes, studied after electrostatic separation. *Z. Phys. A* **340**, 225–226 (1991).
[49] D. Schardt *et al.* Alpha decay of neutron-deficient isotopes with $52 \leq Z \leq 55$, including the new isotopes 106te ($T_{1/2} = 60$ μs) and ^{110}xe. *Nucl. Phys. A* **368**, 153 – 163 (1981).
[50] D. De Frenne and A. Negret. Nuclear data sheets for A = 106. *Nucl. Data Sheets* **109**, 943 – 1102 (2008).
[51] G. Audi, F.G. Kondev, Meng Wang, W.J. Huang, and S. Naimi. The nubase2016 evaluation of nuclear properties. *Chin. Phys. C* **41**, 030001 (2017).
[52] W.J. Huang *et al.* The ame2016 atomic mass evaluation (i). evaluation of input data; and adjustment procedures. *Chin. Phys. C* **41**, 030002 (2017).
[53] Meng Wang *et al.* The ame2016 atomic mass evaluation (ii). tables, graphs and references. *Chin. Phys. C* **41**, 030003 (2017).
[54] G. Royer. Alpha emission and spontaneous fission through quasi-molecular shapes. *J. Phys. G* **26**, 1149–1170 (2000).
[55] Hongfei Zhang *et al.* α decay half-lives of new superheavy nuclei within a generalized liquid drop model. *Phys. Rev. C* 74, 017304 (2006).
[56] H. F. Zhang and G. Royer. Theoretical and experimental α decay half-lives of the heaviest odd-z elements and general predictions. *Phys. Rev. C* **76**, 047304 (2007).
[57] G. Royer and H. F. Zhang. Recent α decay half-lives and analytic expression predictions including superheavy nuclei. *Phys. Rev. C* **77**, 037602 (2008).
[58] Y. Z. Wang, H. F. Zhang, J. M. Dong, and G. Royer. Branching ratios of α decay to excited states of even-even nuclei. *Phys. Rev. C* **79**, 014316 (2009).
[59] H. F. Zhang and G. Royer. α particle preformation in heavy nuclei and penetration probability. *Phys. Rev. C* **77**, 054318 (2008).
[60] Jun-Gang Deng and Hong-Fei Zhang. Analytic formula for estimating the α-particle preformation factor. *Phys. Rev. C* **102**, 044314 (2020).
[61] J. M. Dong, H. F. Zhang, and G. Royer. Proton radioac-

tivity within a generalized liquid drop model. *Phys. Rev. C* **79**, 054330 (2009).

[62] X J Bao *et al.* Half-lives of cluster radioactivity with a generalized liquid-drop model. *J. Phys. G* **39**, 095103 (2012).

[63] G. Royer and B. Remaud. Static and dynamic fusion barriers in heavy-ion reactions. *Nucl. Phys. A* **444**, 477 – 497 (1985).

[64] G. Royer and K. Zbiri. Asymmetric fission for 70,76Se and 90,94,98Mo via quasimolecular shapes and related formulas. *Nucl. Phys. A* **697**, 630 – 638 (2002).

[65] Jun-Gang Deng and Hong-Fei Zhang. Correlation between α-particle preformation factor and α decay energy. *Physics Letters B* **816**, 136247 (2021).

[66] H. F. Zhang, G. Royer, and J. Q. Li. Assault frequency and preformation probability of the α emission process. *Phys. Rev. C* **84**, 027303 (2011).

[67] G. L. Zhang, X. Y. Le, and H. Q. Zhang. Calculation of α preformation for nuclei near $N = 162$ and $N = 184$. *Phys. Rev. C* **80**, 064325 (2009).

[68] Jun-Gang Deng *et al.* α decay properties of ^{297}Og within the two-potential approach. *Chin. Phys. C* **41**, 124109 (2017).

[69] Jun-Gang Deng *et al.* α decay properties of ^{296}Og within the two-potential approach. *Chin. Phys. C* **42**, 044102 (2018).

[70] Ning Wang, Min Liu, Xizhen Wu, and Jie Meng. Surface diffuseness correction in global mass formula. *Phys. Lett. B* **734**, 215–219 (2014).

[71] Saad M Saleh Ahmed *et al.* Alpha-cluster preformation factors in alpha decay for even–even heavy nuclei using the cluster-formation model. *J. Phys. G* **40**, 065105 (2013).

[72] M. Hasegawa and K. Kaneko. Microscopic analysis of T=1 and T=0 proton-neutron correlations in N=Z nuclei. *Nucl. Phys. A* **748**, 393 – 401(2005).

[73] Xiao-Dong Sun, Ping Guo, and Xiao-Hua Li. Systematic study of favored α-decay half-lives of closed shell odd-a and doubly-odd nuclei related to ground and isomeric states. *Phys. Rev. C* **94**, 024338 (2016).

[74] Jun-Gang Deng *et al.* Systematic study of unfavored α-decay half-lives of closed-shell nuclei related to ground and isomeric states. *Phys. Rev. C* **96**, 024318 (2017).

[75] Jun-Gang Deng *et al.* Systematic study of α decay of nuclei around the $Z = 82, N = 126$ shell closures within the cluster-formation model and proximity potential 1977 formalism. *Phys. Rev. C* **97**, 044322 (2018).